

Water–mucin phases: conditions for mucus liquid crystallinity¹

Jonathan M. Davies, Christopher Viney*

Department of Materials, University of Oxford, Parks Road, Oxford OX1 3PH, UK

Abstract

Previous studies of mucin conformation in aqueous media have focussed on the polymer backbone, on dilute concentrations, and on ambient temperatures. Using differential scanning calorimetry and transmitted polarised light microscopy, we demonstrate that commercially available pig gastric mucin forms a liquid crystalline gel at concentrations above approximately 26% w/w in water. Solvated mucin exhibits a glass transition at approximately 24.8°C, and the liquid crystalline phase is only fluid above this temperature. We associate the glass transition with the onset of flexibility in the backbone of glycosylated molecular segments. Consideration of molecular geometry suggests that mucin liquid crystallinity is governed by interactions between side chains, not main chains. For mucin from a given source, neither the conditions required for liquid crystallinity nor the glass transition temperature should be sensitive to the mucin molecular weight, as long as the integrity of the glycosylated segments is maintained. We consider some physiological implications of our results, including the impact of hypothermic conditions on the functionality of mucus, and we emphasise the need to characterise mucin and mucus structure at physiological temperatures. © 1998 Elsevier Science B.V.

Keywords: Mucin; Mucus; Liquid crystal; Phase diagram; Differential scanning calorimetry

1. Introduction

Mucus performs many specialised roles in the animal kingdom [1–4]. Its barrier and transport properties are essential to proper functioning of the digestive, respiratory and reproductive systems of vertebrates, including humans. Invertebrates use mucus as an external surface coating to reduce friction or hydrodynamic drag, to provide a barrier against infection, and to limit water loss; in addition, mucus can serve as an aid in locomotion and navigation, a snare for prey, a mating rope, or a ‘scaffolding’ that provides anchorage and protection for eggs. From an engineering point of view, mucus is an outstanding water-based lubricant: giraffes can use their sensitive

tongues to strip the foliage from thorny acacia trees, and slugs can crawl unharmed over a new razor blade.

The principal components of mucus are mucin and water. The glycoprotein mucin forms the macromolecular matrix of mucus and dominates its rheological properties. Mucin has a linear protein backbone; some segments of this backbone are rich in the amino acids serine and threonine, and are heavily glycosylated with O-linked oligosaccharide side chains (Fig. 1). While it has long been held that the oligosaccharides contain approximately 20 (but up to 30) monomer units each [5], it has recently been observed that this number may be as high as 100 [6]. The relatively rigid, heavily glycosylated segments alternate with relatively flexible segments that are free of carbohydrate.

In dilute aqueous solution, the more flexible segments allow mucin to adopt an isotropic coil conformation, so that individual molecules occupy a spherical domain in the solvent. The sphere radius

*Corresponding author. Fax: +44 1865 273794; e-mail: christopher.viney@materials.ox.ac.uk

¹Presented at TAC 97, Oxford, UK, 14–15 April 1997.

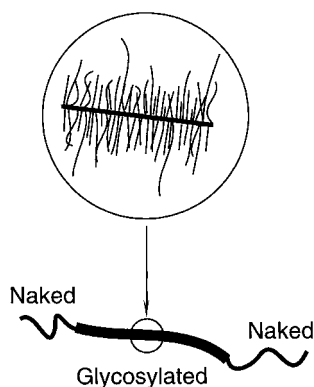


Fig. 1. Schematic illustration of mucin basic unit, consistent with several sources [5,16,18,19]. Whole mucin can be regarded as a copolymer of relatively rigid (glycosylated) and relatively flexible (naked) moieties.

is expanded significantly relative to the value that would be associated with a strictly random backbone conformation; in part this reflects the presence of the rigid segments. It is possible for the spheroidal domains of whole mucin to overlap at concentrations approaching 1% w/w, corresponding to the onset of gel formation [5]. While a variety of techniques have been used to characterise mucin conformation, such studies have been limited to concentrations below the critical value for gelation; typically, concentrations up to 4 mg/ml have been used [5,7]. As a result of these studies, it has become accepted that the macromolecular matrix in mucus is isotropic at all length scales (except at the level of individual, rigid, heavily glycosylated segments).

By extension, this model is applied implicitly to the condensed state of as-secreted mucins. The molecular volume of mucin differs drastically between the decondensed and (re-)condensed states, but the transition is not expressed in terms of significant changes in secondary structure, tertiary structure, intramolecular order or intermolecular order. Instead, mechanisms of decondensation and (re-)condensation are described in terms of the charge density of the polyionic mucin molecule, the degree of electrostatic shielding of the polyionic charges, and the dielectric constant of solvent and non-solvent species present [8]. Yet, given the explosive rate at which as-secreted slug mucin granules can swell (the volume can increase by a factor of 600 in 40 ms), it follows that the condensed

mucin must have been folded in an orderly way that facilitates unobstructed expansion [9].

Direct evidence that mucin can have different packing schemes in the decondensed and (re-)condensed states was provided by observations that concentrated mucus exhibits liquid crystalline microstructures [10,11]. Liquid crystallinity implies the presence of orientationally ordered, rod-like moieties [12]: their existence in the condensed state of mucin would in turn ease the rapid, unrestricted unfolding of the as-secreted mucin polymer network. Initial molecular-level interpretation of mucus liquid crystallinity noted that the sequence of rigid and flexible backbone segments in mucin is analogous to the configuration of main chain liquid crystal polymers in which rigid units alternate with flexible moieties. However, there is another way in which molecules with the configuration of mucin could form a liquid crystalline phase: domains of orientationally ordered side chains could develop at sufficiently high concentrations. In the present paper, we discuss evidence that mucin is indeed a side chain liquid crystal polymer, and we determine the conditions of concentration and temperature at which the liquid crystalline phase is formed.

2. Experimental

2.1. Materials

The ability of mucus to develop liquid crystalline order has been demonstrated in both *Ariolimax columbianus* (slug) pedal mucus and human tracheal mucus [10,11]. The slug mucus can be collected without the contaminants unavoidably associated with vertebrate mucus. In either case, however, it is difficult to prepare specimens of known mucin content reproducibly, because the concentration of the as-collected mucus cannot be measured accurately. For this reason, and also to ensure ready availability of adequate sample volumes, we chose to work with commercially available lyophilised porcine gastric mucin.

The product used was type III mucin (partially purified [13] from porcine stomach), containing 1% bound sialic acids (Sigma, St. Louis, MO, USA; cat. no. M1778, lot no. 104H7175). The solvent was distilled water, containing 0.1% w/w sodium azide

to combat microorganism growth. Saline, Ringer's, or buffered solutions were not used, so that results could be referred appropriately to the context of a binary phase diagram, and so that microstructures were not complicated by the deposition of salt crystals. Samples of the desired concentration (% w/w) could be prepared easily by weighing out a known amount of the dry mucin and adding the appropriate volume of solvent. Given the imperfect homogeneity of the commercial mucin (see below), we were able to approximate the density of the 0.1% w/w sodium azide solution as 1000 kg m^{-3} with negligible effect on the accuracy of our results.

2.2. Methods

2.2.1. Determining the solubility of commercial lyophilised mucin

As-received mucin was weighed into tared 1.5 ml Eppendorf (microcentrifuge) tubes. The amount used was always slightly less than that needed to yield a full tube after addition of solvent. A micropipette was used to add sufficient 0.1% w/w sodium azide solution to give nominal mucin concentrations of either 0.5 or 2% w/w. (Higher concentrations were avoided, because they exhibited incomplete separation on subsequent centrifugation. This characteristic coincides with the onset of gel formation, which, because the commercial extraction/purification process degrades the mucin molecular weight [14], is displaced to concentrations higher than the critical value of around 1% referred to in Section 1.)

Samples were spun at 15 000 revolutions per minute for 3 min in a microcentrifuge (Heraeus Biofuge model 15, Heraeus Instruments GmbH, Osterode, Germany) so that undissolved solid formed a pellet. The supernatant was removed with a micropipette and discarded. The pellets were washed with 1 ml ice cold 70% ethanol and re-centrifuged at 15 000 rpm for 3 min, after which the supernatant was removed and discarded. Pellets, still in the Eppendorf tubes, were dried for 10 min in a heated SpeedVac (Savant, Holbrook, NY, USA; model SC110A-200). The amount of undissolved solid was determined by weighing.

2.2.2. Preparation of stock gels

Mucin/solvent gels for characterisation by differential scanning calorimetry (DSC) and transmitted

polarised light microscopy were prepared and stored in 10 ml glass vials equipped with plastic lids and sealed with Parafilm. Nominal sample compositions (i.e. before correcting for insoluble material) were in increments of 5% w/w, starting at 5% w/w. The samples were left to equilibrate for several days; control weighings determined that there was no significant water loss from the vials. Equilibrated samples appeared homogeneous to the unaided eye and through a hand-held magnifier, and exhibited a uniform colour. As judged by this test, it was not possible to prepare equilibrated mixtures above a nominal solids concentration of 65% w/w, so these compositions were not subjected to further characterisation.

2.2.3. Differential scanning calorimetry

A Perkin Elmer DSC7 equipped with an Intracooler 1 and drybox was used to identify phase transitions, and to obtain quantitative thermodynamic data associated with those transitions. The calorimeter was calibrated with indium reference material according to manufacturer's instructions. Samples were sealed hermetically into 25 μl aluminium pans, and left to re-equilibrate for at least 1 h. They were heated from 15 to above 100°C at $10^\circ\text{C min}^{-1}$. The purge gas was dry argon, flowing at 30 ml min^{-1} . Data were analysed with manufacturer's software.

In principle, light microscopy could be used instead of DSC to determine the temperature at which a liquid crystalline phase is stable. However, aside from the fact that DSC offers a substantially quicker route to identifying these temperatures, it also provides numbers that are more reliable. The limitations of microscopy in this respect arise because (a) optically resolvable domains of the new phase have to form before the transition is detectable with the microscope, and (b) the scale and nature of liquid crystalline microstructures are sensitive to specimen–substrate interactions which may not be exactly reproducible from one preparation to the next [15]. We believe that this is the first published account of DSC being applied to mucus characterisation.

2.2.4. Transmitted polarised light microscopy

Each equilibrated sample for microscopy was confined between a glass microscope slide ($75\times$

25 × 1 mm; VWR Scientific, San Francisco, CA, USA) and cover glass (no. 1 $\frac{1}{2}$, 22 mm square; Corning Glass Works, Corning, NY, USA). Glassware was washed in household detergent solution, rinsed in distilled water, rinsed in ethanol (absolute alcohol, A.R. quality), air dried, and stored in a desiccator until needed. The edges of the cover glass were sealed with silicone grease (M494, Ambersil, Bridgwater, UK). This grease was specifically chosen for its immiscibility with and inertness towards water (it is approved for use with potable water), so that any inadvertent contact with the specimen would not lead to contamination. Control weighings conducted over a period of one month determined that no significant water loss occurred from confined samples at ambient temperature.

An Ultraphot II light microscope (Carl Zeiss, Oberkochen/Württemberg, Germany), equipped with a xenon arc lamp and crossed polars, was used in transmission to characterise sample microstructures. The xenon arc lamp was necessary to obtain good contrast from liquid crystalline samples. Images were recorded on 35 mm film (400 ASA for optimal contrast). A Linkam THMS 600 heating/freezing stage and TP 92 temperature programmer/controller (Linkam Scientific Instruments, Tadworth, Surrey, UK) were used to observe sample microstructures at physiological temperatures.

3. Results and discussion

3.1. Mucin solubility

It is well known that the molecular weight of mucin is highly sensitive to the techniques used in collection and handling [16–19]. In the case of gastric mucin, retained enzyme impurities may become activated by the solvent used for extraction and handling; enzymatic attack at ‘naked’ stretches of backbone protein can then yield mucin fragments rather than whole mucin. On the other hand, operations typically used in purification protocols, for example stirring, pipetting, sonication, high-speed homogenisation, and lyophilisation can also degrade molecular weight. Furthermore, high concentrations of reagents (CsCl, guanidinium chloride) used in density gradient centrifugation will denature mucins and irreversibly

affect their rheological behaviour – as will the removal of non-covalently bound components. The functionality of mucin can therefore be compromised regardless of whether or not it is purified!

In the present experiments, we elected to work with the as-received commercial product, on the basis that additional purification would further degrade molecular weight and alter functionality relative to the native condition. The fact that we are able to redissolve a majority fraction of the lyophilised commercial product indicates that the macromolecules have already undergone significant molecular weight degradation [16]. Quantitatively, this degradation has been demonstrated by a combination of size exclusion chromatography and multi angle laser light scattering [14]: the commercial product was found to have a weight-average molecular weight of 1.25×10^6 , while the value for fresh mucin (also partially purified) was 4.72×10^6 . These averages reflect the presence of any small molecule impurities as well as the distribution of mucin molecular sizes. In comparison, the molecular weight of a basic unit (a single highly glycosylated backbone region and one or two naked backbone regions) is approximately 0.5×10^6 . The extent of molecular weight degradation in the as-received commercial product limits its suitability as a model compound for studying mucin rheological and bioadhesive properties. However, the principal conclusions of this paper – concerning mucin as a side chain lyotropic polymer – should not be sensitive to backbone molecular weight [20].

We found that the fraction dissolved did not increase measurably at 37°C relative to the solubility at ambient temperature, even after heating for several days, which suggests that our samples do not experience significant degradation by enzyme impurities. For the nominally 0.5% w/w samples, $73 \pm 12\%$ of the as-received mucin went into solution (average and standard deviation for five measurements). In the case of the nominally 2% w/w samples, the soluble fraction of as-received mucin was $81 \pm 1\%$ (again based on five measurements). The larger variability obtained with the more dilute samples shows that the as-received mucin powder has a markedly non-uniform solubility. Concentrations of solvated material therefore will be more reliable if larger volumes of solution or gel are prepared – hence our choice of 10 ml stock gel vials, even though subse-

quent characterisation required only 50 μl of each composition.

3.2. Transmitted polarised light microscopy at ambient temperature

Given the successful observation of liquid crystalline textures in slug and human tracheal mucus at ambient temperatures [10,11], we examined equilibrated samples by transmitted polarised light microscopy. No evidence of liquid crystallinity was seen, at any of the sample concentrations. With the polariser and/or analyser withdrawn, it was possible to observe the insoluble component of the as-received mucin; the fraction of the field of view occupied by these irregular particles increased in proportion to the nominal concentration of the samples. At the resolution afforded by a $40\times$ ($\text{NA}=0.85$) objective, it was also apparent that the nominally 65% w/w gel was not in fact homogeneous; we therefore did not perform further characterisation on this gel.

The equilibrated samples described in the present paper were prepared by a very different route, compared to the slug pedal mucus and human tracheal mucus specimens exhibiting liquid crystallinity in our previous work. Instead of adding water to dry mucin, we previously started with dilute mucus of unknown quantitative concentration and allowed water to evaporate until liquid crystalline microstructures were seen. In those experiments, we also noted that the initial qualitative concentration and the drying rate determined whether or not a liquid crystalline phase was ever observed [11]. In our present study, we therefore monitored initially equilibrated samples that were allowed to become more concentrated by evaporation at several different rates. The highest drying rates were achieved by placing material on a glass microscope slide with no cover slip, while the lowest rates were achieved by omitting the silicone grease seal from the microscope slide/cover slip sandwich and placing samples together with damp tissue paper in a small Tupperware box. Liquid crystalline textures were not observed at any stage in any of the drying samples. Instead, supersaturated samples precipitated crystalline solid, with a fern-like morphology [10] being formed at the highest drying rates.

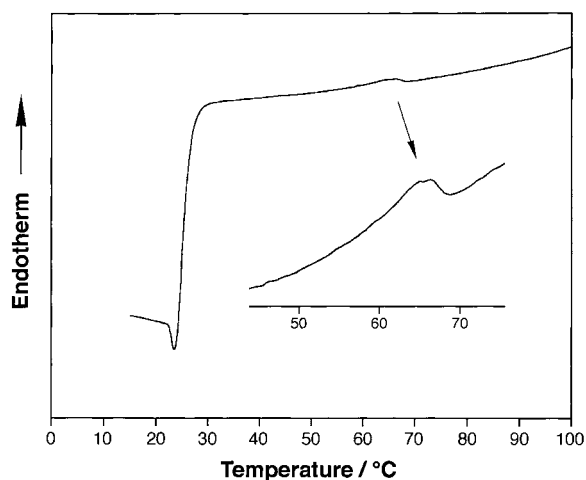


Fig. 2. DSC trace obtained on heating a 28.4% w/w mucin gel (nominal composition 35% w/w before correcting for mucin solubility) at $10^\circ\text{C min}^{-1}$. Inset: endotherm, with horizontal and vertical scales expanded respectively by factors of 1.5 and 7 relative to the main Figure.

3.3. Differential scanning calorimetry and transmitted polarised light microscopy at above-ambient temperatures

3.3.1. Identification of transitions

A typical DSC scan for hydrated mucin is shown in Fig. 2. Its principal features, in ascending order of temperature, are a well-defined exotherm, a glass transition, and a broad endotherm. Figs. 3–6 show data derived from the DSC scans; each Figure is plotted versus sample concentration which has been corrected to account for insoluble material. From Fig. 3, we note that the range of pig body temperatures [21] ($39.0\text{--}40.3^\circ\text{C}$) lies above the T_g end temperature at all concentrations studied. Figs. 4–6 consistently point to a transition occurring in the gels in the concentration range 20.3–28.4% w/w. Cricket Graph v.1.3.2 (Cricket Software, Malvern, PA, USA) was used to fit a pair of straight lines to the data in each plot, to estimate the concentration at which the transition occurs. We emphasise that this construction provides only approximate values of the critical concentration, as there is no theoretical basis for assuming straight line correlations on any of the plots. In deciding that the 20.3% w/w data point lies below the transition, while the 28.4% w/w data point lies

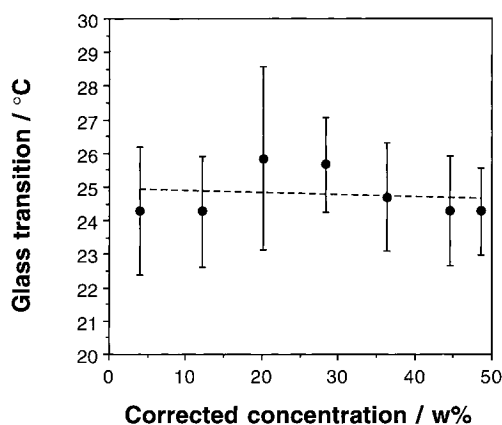


Fig. 3. Values of T_g as a function of mucin gel concentration. Data were derived from DSC traces obtained on heating at $10^\circ\text{C min}^{-1}$. Ranges from T_g onset temperature to T_g end temperature are shown as vertical bars.

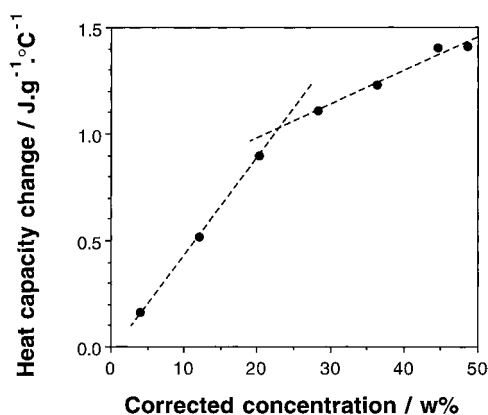


Fig. 4. Heat capacity change (per gram of mucin) at T_g , plotted as a function of gel concentration. Data were derived from DSC traces obtained on heating gels at $10^\circ\text{C min}^{-1}$.

above the transition, we were guided by our observations made by light microscopy (see below).

A DSC trace for dry as-received mucin is shown in Fig. 7. The material undergoes an exothermic transition in the same temperature range as the hydrated samples, but this is followed by a decrease rather than an increase in heat capacity. There is no longer an obvious glass transition, and there is no evidence of the endothermic transition seen in the gels. We do not include quantitative data from Fig. 7 in Figs. 3–6, because the opportunities for molecular aggregation/interaction that arise in the presence of solvent

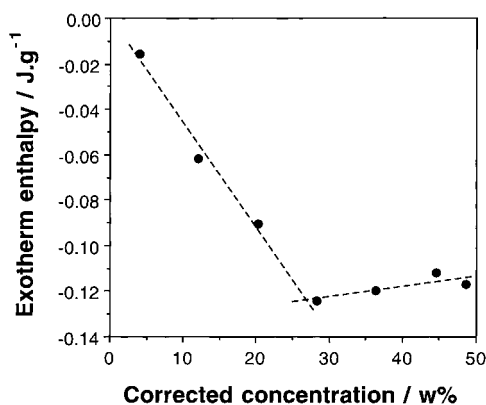


Fig. 5. Enthalpy change (per gram of mucin) for the pre- T_g exotherm, plotted as a function of gel concentration. Data were derived from DSC traces obtained on heating gels at $10^\circ\text{C min}^{-1}$.

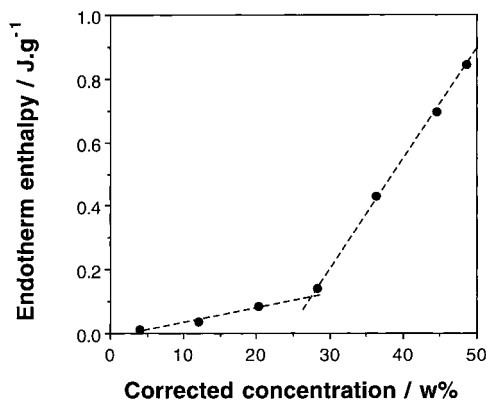


Fig. 6. Enthalpy change (per gram of mucin) for the endotherm above T_g , plotted as a function of gel concentration. Data were derived from DSC traces obtained on heating gels at $10^\circ\text{C min}^{-1}$.

are not available in the dry material, so the quantitative thermodynamic data are not directly comparable.

Light microscopy revealed that the gels of corrected concentration equal to or greater than 28.4% w/w (nominal concentration 35% w/w) formed a stable liquid crystalline phase on heating to above T_g but below the onset of the endotherm. A typical liquid crystalline texture is shown in Fig. 8. The textures were diffuse, as is often the case for viscous liquid crystalline polymer solutions and gels – for example, lyotropic liquid crystalline polysaccharides [22–24]. While image sharpness can be improved by decreasing the specimen thickness, we did not want to induce molecular alignment artificially by pressing down on

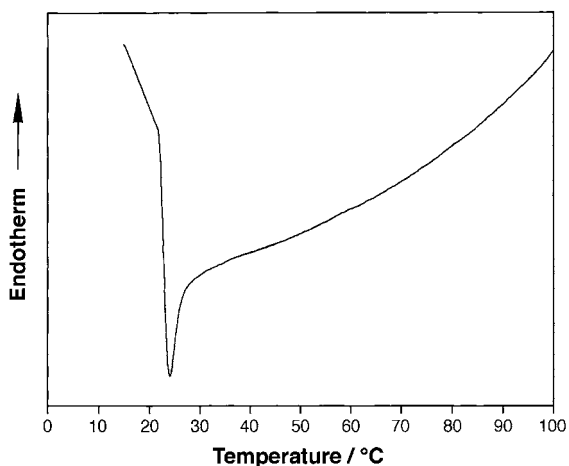


Fig. 7. DSC trace obtained on heating as-received lyophilised mucin at $10^{\circ}\text{C min}^{-1}$.

the cover slip. We were able to preserve liquid crystalline microstructures at room temperature, and thus characterise them at higher resolution than permitted by the heating stage, by cooling samples to below T_g on a cold metal surface. Samples heated into the range of temperatures covered by the endotherm became biphasic, exhibiting a mixture of isotropic and liquid

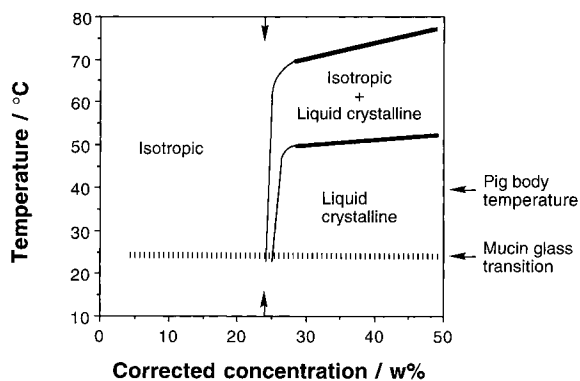


Fig. 9. Partial phase diagram for water/mucin, derived from DSC and polarised light microscopy data.

crystalline regions; the amount of isotropic material increased to 100% on heating past the upper limit of the endotherm.

Fig. 9 shows a phase diagram constructed from our DSC and transmitted polarised light microscopy observations. The position of the two bold lines was determined from the extent of the endotherm on DSC traces. The position of the thin lines is approximate; they fulfil the necessary conditions

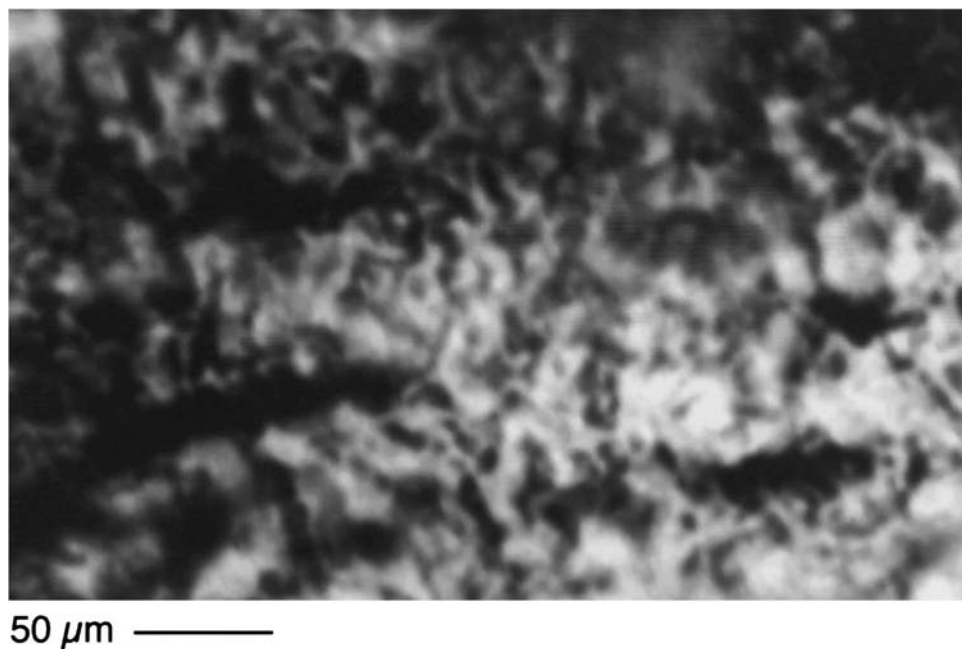


Fig. 8. Transmitted polarised light micrograph of 48.6% w/w mucin gel quenched to ambient temperature from 50°C .

of (a) connecting to the bold lines, (b) lying to the right of the optically isotropic 24.3% w/w sample (concentration marked by short vertical arrows), and (c) consistency with the topology of phase diagrams [25] for a lyotropic polymer/solvent binary system.

3.3.2. *Origins of mucin liquid crystallinity*

The fact that the mucin backbone contains both rigid and flexible segments makes it a potential main chain liquid crystal polymer – as noted in Section 1 and in previous publications [10,11]. In this model, the flexible segments would increase entropy and confer solubility, while the rigid segments would provide geometrical anisotropy needed to promote liquid crystallinity. The rigid segments would need to have an axial ratio (length-to-width ratio) in excess of ~ 6.7 for a liquid crystalline phase to form [26]. However, it is unlikely that the rigid segments have an axial ratio that is as high as this critical value, as is demonstrated by the following ‘back-of-the-envelope’ calculation.

The heavily glycosylated segments extend for approximately 100 nm [18]. If we take the side chains as containing up to 30 monosaccharides each [5], we can use 1 nm as an illustrative disaccharide repeat distance [27] to estimate the side chain length as approximately 15 nm, and therefore the glycosylated segment diameter as approximately 30 nm. This would give an axial ratio of approximately 3.3. In estimating the side chain length, we have assumed an extended conformation. A departure from this conformation sufficient to halve the side chain length would be needed to achieve an axial ratio of 6.7. However, steric interactions within the ‘coat’ of side chains [28] are likely to promote near-extended conformations. In addition, it has been shown recently that carbohydrate chains in pig gastric mucin may contain up to 100 sugars [6], which would lead to an axial ratio as low as 1 for the heavily glycosylated segments.

Two further considerations work against mucin being a main chain liquid crystalline polymer. First, the polydispersity of the oligosaccharides will preclude the heavily glycosylated segments from having a smooth envelope, which in turn will diminish their ability to pack into liquid crystalline domains. Second, the critical axial ratio of 6.7 needed

for liquid crystallinity is a limiting value for a system consisting of rods only (100% w/w concentration). The fact that we observe mucin as being fully (single-phase) liquid crystalline at a concentration as low as 28% w/w suggests that the axial ratio of typical rigid segments must be of the order of 20–30 [29]. This range would however be consistent with typical axial ratios of conformationally extended side chains in mucin.

In the following sections, we discuss the quantitative data that we derived from our DSC characterisation of mucin gels, consistently interpreting the results in the context of mucin as a side chain liquid crystalline polymer. This model depends on the integrity of the mucin basic units, but not on their polymerisation into subunits or whole mucin, so the molecular weight degradation [14] that occurs in preparing the commercial mucin used in our studies should not affect our conclusions.

3.3.3. *Glass transition and associated change in heat capacity*

The glass transition (Fig. 3) is approximately constant (average 24.8°C) over the entire range of corrected compositions up to 48.6% w/w, i.e. for all concentrations at which homogeneous specimens could be prepared. Since the polymer is solvated by water at temperatures below T_g , it is improbable that T_g corresponds to the entire main chain becoming flexible; it is in any case widely accepted that the naked segments of mucin are flexible under ambient conditions. At the same time, the glass transition is too marked to be just the consequence of side chains gaining conformational mobility. Instead, we assign the transition to the onset of flexibility in the backbone of the heavily glycosylated segments. The effective length of the segments becoming flexible at T_g will be determined by the extent of the individual heavily glycosylated segments, and not by the density of cross-links (mechanical or chemical) involving the already flexible naked regions. This is consistent with the transition remaining approximately independent of concentration. For the same reason, we do not expect overall molecular weight to significantly affect T_g , as long as the integrity of the heavily glycosylated segments is not compromised. The length of the heavily glycosylated segments is under genetic control, and so should be monodisperse, leading to the

observed narrow range between the T_g onset and end temperatures.

As the heavily glycosylated segments acquire conformational mobility, the number of conformations accessible to the already flexible, naked segments will increase too. The change in the number of conformationally accessible states, per segment, will be more marked for greater incidences of chain interaction, regardless of whether the interactions are due to cross links between naked regions of backbone or due to the isotropic coils becoming more compact as concentration increases. Thus the accompanying increase in heat capacity per unit mass of polymer will be greater at higher polymer concentrations.

There is another factor to consider. When the system becomes liquid crystalline above the critical mucin concentration, the development of orientational order between side chains imposes a small reduction in the number of possible backbone conformations, compared to the number accessible in the isotropic state [20]. Thus, while the heat capacity change at T_g , per unit mass of polymer, can continue to increase with concentration in the liquid crystalline state, the rate of increase will not be as high as in the isotropic state. Qualitatively, this picture agrees with the data shown in Fig. 4.

3.3.4. Exotherm immediately preceding the glass transition

The ability of side chains to participate in the favourable interactions needed for liquid crystal formation will initially increase as the concentration of molecules increases. Since we are concerned with intermolecular interactions, an exotherm associated with these interactions will be characterised by an enthalpy per unit mass of polymer that initially increases with polymer concentration, as seen in Fig. 5. Because the ability of side chains to interdigitate optimally will depend on the local flexibility of the backbone segments to which they are attached, the endotherm will be closely linked to the glass transition.

When the concentration is sufficiently high to effect the formation of a liquid crystalline phase, the capacity of each molecule's side chains to align with the side chains of neighbouring molecules is saturated. There is consequently little change in enthalpy per unit

mass of polymer at concentrations beyond that needed for liquid crystallinity (Fig. 5).

Fig. 7, obtained from dry mucin, is dominated by the exotherm under discussion. The exotherm occurs at the same temperature as in the case of the gels, and is therefore presumed to result from the same type of side chain interactions. But, the absence of solvent now denies the main chains sufficient free volume to access the conformations that should become available with increasing temperature. Instead, the favourable side chain interactions act effectively as cross-links, so that heat capacity decreases on heating dry mucin through the temperature range where T_g occurs in the gels. The lack of microstructural mobility persists on heating, so that dry mucin does not exhibit a fluid liquid crystalline phase or a transition to an isotropic phase. The material starts to degrade significantly at approximately 105°C.

3.3.5. Endotherm above the glass transition

From our polarised light microscopy observations of liquid crystalline samples, we deduce that this endotherm represents the enthalpy needed to fully isotropise the mucin gels.

Below the critical concentration for liquid crystallinity, the enthalpy per unit mass of polymer increases with concentration (Fig. 6) as the molecules are increasingly able to develop favourable side chain interactions above T_g . Local 'domains' of side chain orientational order, in an otherwise isotropic environment, are destroyed on heating through the endotherm. These 'domains' are too small and localised to be resolved by light microscopy, and specimens are optically isotropic.

Above the critical concentration, samples are globally liquid crystalline, with order being imposed on the main chains as well as existing between side chains. The macromolecules pack ever more densely as concentration increases further, and the isotropisation enthalpy per unit mass of polymer changes with concentration at a higher rate than before.

3.3.6. Some physiological considerations

Our results suggest that as-secreted granules of pig gastric mucin will pass through a liquid crystalline regime as they undergo swelling. Because liquid crystalline phases are usually associated with a reduction in viscosity [30], there may be significant impli-

cations concerning the ability of mucus to coat the stomach. We have remarked above that the range of pig body temperatures lies above the mucin gel T_g end temperature at all concentrations studied. However, given that the mechanical and rheological properties of polymer networks are especially sensitive to temperature in the vicinity of T_g , it is apparent that hypothermic conditions could have serious consequences for the formation of functional mucus. Also, the noticeable thickening of mucus that can temporarily follow consumption of an ice cold beverage may be related to the mucus having cooled towards its T_g .

An obvious extension of our work will involve below-ambient scanning calorimetry of slug pedal mucus and human tracheal mucus, both of which have been shown previously [10,11] to form liquid crystalline phases at ambient temperature. These two types of mucus do have to function at or close to ambient temperature: slugs are poikilothermic, and, though humans are homeothermic, the surface temperature of tracheal mucus may approach the temperature of the air being breathed. On the basis of what we have observed in the present study, both the pedal and tracheal mucus may exhibit a T_g below ambient temperatures, if the water does not freeze first.

4. Conclusions

Mucin is a lyotropic side chain liquid crystal polymer. In the case of aqueous gels of commercially available pig stomach mucin, the critical concentration for liquid crystallinity lies between 24% w/w and 28% w/w. The results obtained by analysing three different features on DSC traces average to 26% w/w as a close estimate of the critical concentration.

When solvated, the commercially available pig stomach mucin exhibits a glass transition at approximately 24.8°C. A fluid liquid crystalline phase is only formed above this temperature. The functionality of mucus may be compromised under hypothermic conditions.

Depending on the material source, characterisation of mucin and mucus at ambient temperatures may not yield results that are representative of properties at physiological temperatures.

Acknowledgements

We are grateful to Dr. L. Gilliland (Sir William Dunn School of Pathology, University of Oxford) for practical help with the characterisation of mucin solubility. We also acknowledge the tutorial contribution of Prof. P. Verdugo (Center for Bioengineering, University of Washington), as well as helpful information provided by Dr. S. Harding (Dept. of Applied Biochemistry and Food Science, University of Nottingham) and Dr. J. Hutchinson (Dept. of Engineering, University of Aberdeen).

References

- [1] T.L. Daniel, *Biol. Bull.* 160 (1981) 376.
- [2] E. Chantler, N.A. Ratcliffe (Eds.), *Mucus and Related Topics*, Society for Experimental Biology, Cambridge, UK, 1989.
- [3] M.W. Denny, in: E. Chantler, N.A. Ratcliffe (Eds.), *Mucus and Related Topics*, Society for Experimental Biology, Cambridge, UK, 1989, p. 337.
- [4] E.A. Koch, R.H. Spitzer, R.B. Pithawalla, *J. Struct. Biol.* 106 (1991) 205.
- [5] S.E. Harding, *Adv. Carbohydr. Chem. Biochem.* 47 (1989) 345.
- [6] C.J. Roberts, A. Shivji, M.C. Davies, S.S. Davis, I. Fiebrig, S.E. Harding, S.J.B. Tendler, P.M. Williams, *Protein Peptide Lett.* 2 (1995) 409.
- [7] S.E. Harding, A.J. Rowe, J.M. Creeth, *Biochem. J.* 209 (1983) 893.
- [8] P. Verdugo, *Annu. Rev. Physiol.* 52 (1990) 157.
- [9] P. Verdugo, I. Deyrup-Olsen, A.W. Martin, D.L. Luchtel, in: E. Karalis (Ed.), *Swelling of Polymer Networks*, Springer, Heidelberg, 1992, p. 671.
- [10] C. Viney, A. Huber, P. Verdugo, *Macromolecules* 26 (1993) 852.
- [11] C. Viney, A. Huber, P. Verdugo, in: C. Ching, D.L. Kaplan, E.L. Thomas (Eds.), *Biodegradable Polymers and Packaging*, Technomic, Lancaster, PA, 1993, p. 209.
- [12] S. Chandrasekhar, *Liquid Crystals*, Cambridge University Press, Cambridge, 1992.
- [13] D.A. Glenister, K.E. Salamon, K. Smith, D. Beighton, C.W. Keevil, *Microbial Ecol. Health Dis.* 1 (1988) 31.
- [14] K. Jumel, I. Fiebrig, S.E. Harding, *Int. J. Biol. Macromol.* 18 (1996) 133.
- [15] C. Noël, in: A.A. Collyer (Ed.), *Liquid Crystal Polymers: From Structures to Applications*, Elsevier, London, 1992, p. 31.
- [16] I. Carlstedt, J.K. Sheehan, in: J. Nuget, M. O'Connor (Eds.), *Mucus and Mucosa*. Ciba Foundation Symposium 109, Pitman, London, 1984, p. 157.
- [17] H.S. Slayter, G. Lamblin, A. Le Treut, C. Galabert, N. Houdret, P. Degand, P. Roussel, *Eur. J. Biochem.* 142 (1984) 209.

- [18] I. Carlstedt, J.K. Sheehan, in: E. Chantler, N.A. Ratcliffe (Eds.), *Mucus and Related Topics*, Society for Experimental Biology, Cambridge, UK, 1989, p. 289.
- [19] R. Bansil, E. Stanley, J.T. LaMont, *Annu. Rev. Physiol.* 57 (1995) 635.
- [20] H. Finkelmann, in: A. Ciferri (Ed.), *Liquid Crystallinity in Polymers: Principles and Fundamental Properties*, VCH, New York, 1991, p. 315.
- [21] P.L. Altman, D.S. Dittmer (Eds.), *Metabolism (Biological Handbooks)*, Federation of American Societies for Experimental Biology (FASEB), Bethesda, MD, 1968, p. 328.
- [22] C. Viney, A.H. Windle, *Liq. Cryst.* 1 (1986) 379.
- [23] A.E. Huber, P.S. Stayton, C. Viney, D.L. Kaplan, *Macromolecules* 27 (1994) 953.
- [24] C. Viney, W.S. Putnam, *Polymer* 36 (1995) 1731.
- [25] S.P. Papkov, *Adv. Polym. Sci.* 59 (1984) 75.
- [26] P.J. Flory, *Macromolecules* 11 (1978) 1141.
- [27] W.T. Astbury, *Nature* 155 (1945) 667.
- [28] A. Silberberg, in: E. Chantler, N.A. Ratcliffe (Eds.), *Mucus and Related Topics*, The Society for Experimental Biology, Cambridge, UK, 1989, p. 43.
- [29] M. Warner, P.J. Flory, *J. Chem. Phys.* 73 (1980) 6327.
- [30] M.G. Northolt, D.J. Sikkema, *Adv. Polym. Sci.*, 98 (1990/91) 115.